

# Surface Functionalization Technique for Conferring Antibacterial Properties to Polymeric and Cellulosic Surfaces

Lian Cen, K. G. Neoh,\* and E. T. Kang

Department of Chemical and Environmental Engineering, National University of Singapore, Kent Ridge, Singapore 119260

Received June 23, 2003

A simple surface modification technique was developed to functionalize polymeric and cellulosic materials with bactericidal polycationic groups. The poly(ethylene terephthalate) (PET) film was first graft copolymerized with 4-vinylpyridine (4VP) and subsequently derivatized with hexyl bromide via the quaternization of the grafted pyridine groups into pyridinium groups. The amount of pyridinium groups on the film surface could be controlled by varying the 4VP monomer concentrations used for grafting. The pyridinium groups introduced on the surface of the substrate possess antibacterial properties, as shown by their effect on *Escherichia coli* (*E. coli*). The bacteria killing efficiency is very high when the concentration of pyridinium groups on surfaces is 15 nmol/cm<sup>2</sup> or higher. *E. coli* adhered on the functionalized surfaces are no longer viable when released into an aqueous culture medium. Filter paper, as a typical cellulosic material, was also functionalized in the same manner to introduce the pyridinium groups. The antibacterial activity was also similarly observed for this substrate. Thus, the present surface functionalization method has the advantage of being effective in conferring both polymeric and cellulosic materials with antibacterial properties.

## Introduction

Conferring materials with antibacterial surface properties is a fascinating area for research and development in the battle against microbial contamination. The use of conventional disinfectants or antimicrobial agents is restricted by the toxicity of their residues since they are liquids or gases of low molecular weight.<sup>1</sup> An alternative is the development of polymeric materials with antimicrobial activities and previous studies have shown that cationic polymers with quaternary ammonium groups possess such properties.<sup>2–4</sup> Pioneering work on the properties of pyridinium-type polymers was carried out by Kawabata et al.<sup>5,6</sup> The application of antimicrobial polymers minimizes the environmental problems accompanying the conventional agents, and enhances the efficiency, selectivity, and lifetime of the antimicrobial agents.<sup>7–9</sup> Hence, this approach has good potential for application in the areas related to bioengineering, water treatment, polymeric disinfectants, and environmental protection.

One application of the antibacterial pyridium-type polymers is shown by the work of the MIT/Northeastern group which involves the surface treatment of glass and

commercial polymers with N-alkylated poly(4-vinylpyridine) groups.<sup>10–12</sup> The treated surfaces were shown to be lethal on contact to both gram-positive and gram-negative bacteria, and it was also shown that an N-alkyl chain of six carbon units in length is one of the most effective.<sup>10</sup> However, their method involves a number of chemical reaction steps, which increases the difficulty in controlling the concentration of pyridinium groups on the surface. The method was effective for nonporous surfaces and was not applicable to carbohydrate-based materials, such as paper or clothing. For such materials, another group has developed a technique based on lipophilic alkyl chains.<sup>13,14</sup>

In the present work, we report on a simple two-step technique for functionalizing surfaces with N-hexyl bromide poly(4-vinylpyridine) groups. This technique has the advantage of being effective for both polymeric and carbohydrate-based materials. Poly(ethylene terephthalate) (PET) was chosen as the polymeric substrate to be modified since its excellent physicochemical properties, such as good mechanical strength, good stability in the presence of body fluids and high radiation resistance make it an excellent candidate in biomaterial applications.<sup>15,16</sup> To illustrate the application of this technique to a carbohydrate-based porous material, filter paper was similarly modified.

The approach we developed involves UV-induced surface graft copolymerization of 4-vinylpyridine (4VP), followed by the alkylation of the grafted poly(4-vinylpyridine) with

\* To whom correspondence should be addressed. Telephone: +65 68742186. Fax: +65 67791936. E-mail: chenkg@nus.edu.sg.

(1) Tan, S.; Li, G.; Shen, J.; Liu, Y.; Zong, M. *J. Appl. Polym. Sci.* **2000**, *77*, 1869.

(2) Ikeda, T.; Tazuke, S. *Macromol. Chem., Rapid Commun.* **1983**, *4*, 459.

(3) Ikeda, T.; Yamaguchi, H.; Tazuke, S. *Antimicrob. Agents Chemother.* **1984**, *26*, 139.

(4) Ikeda, T.; Hirayama, H.; Suzuki, K.; Yamaguchi, H.; Tazuke, S. *Macromol. Chem.* **1986**, *187*, 333.

(5) Kawabata, N.; Nishiguchi, M. *Appl. Environ. Microbiol.* **1988**, *54*, 2532.

(6) Kawabata, N.; Inoue, T.; Tomita, H. *Epidemiol. Infect.* **1992**, *108*, 123.

(7) Kenawy, E. R. *J. Appl. Polym. Sci.* **2001**, *82*, 1364.

(8) Kenawy, E. R.; Abdel-Hay, F. I.; El-Shanshoury, A. R.; El-Newehy, M. H. *J. Controlled Release* **1998**, *50*, 145.

(9) Kenawy, E. R.; Abdel-Hay, F. I.; El-Shanshoury, A. R.; El-Newehy, M. H. *J. Polym. Sci., Polym. Chem.* **2002**, *40*, 2384.

(10) Tiller, J. C.; Liao, C.; Lewis, K.; Klivanov, A. M. *PNAS* **2001**, *98*, 5981.

(11) Tiller, J. C.; Lee, S. B.; Lewis, K.; Klivanov, A. M. *Biotechnol. Bioeng.* **2002**, *79*, 465.

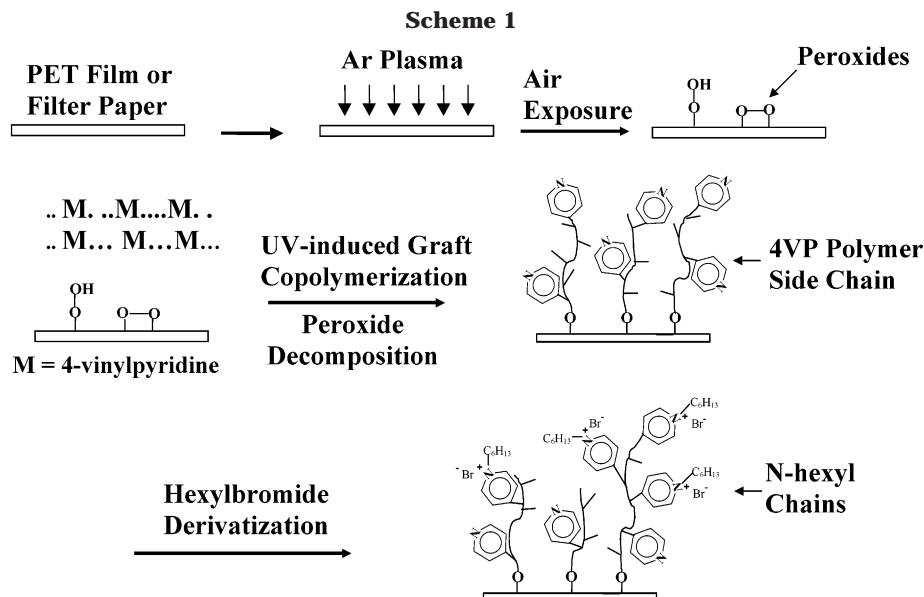
(12) Lin, J.; Tiller, J. C.; Lee, S. B.; Lewis, K.; Klivanov, A. M. *Biotechnol. Lett.* **2002**, *24*, 801.

(13) Abel, T.; Cohen, J. I.; Engel, R.; Filshtinskaya, M.; Melkonian, A.; Melkonian, K. *Carbohydr. Res.* **2002**, *337*, 2495.

(14) Cohen, J. I.; Castro, S.; Han, J.-a.; Behaj, V.; Engel, R. *Heteroatom. Chem.* **2002**, *11*, 546.

(15) Gupta, B.; Plummer, C.; Bisson, I.; Frey, P.; Hilborn, J. *Biomaterials* **2002**, *23*, 863.

(16) Uchida, E.; Uyama, Y.; Ikada, Y. *Langmuir* **1994**, *10*, 481.



hexyl bromide. The manner in which the amount of active groups on the surface of the substrate can be controlled was illustrated and the issues related to the viability and adhesion of the *Escherichia coli* (*E. coli*) bacteria on the functionalized surfaces were investigated.

### Experimental Section

**Materials.** Biaxially oriented poly(ethylene terephthalate) (PET) films of about 100  $\mu\text{m}$  in thickness were purchased from the Goodfellow Inc., Cambridge, U.K. The 4VP monomer of 95% purity, was obtained from Aldrich Chemical Co., Milwaukee, WI, and was freshly distilled under reduced pressure before use. Hexyl bromide, nitromethane and cetyltrimethylammonium chloride were all from Aldrich. Fluorescein (Na salt) was purchased from Sigma Chemical Co. Peptone, yeast extract, agar, and beef extract were purchased from Oxoid. Filter papers of No.1 Grade were obtained from Whatman Co. *E. coli* was obtained from American Type Culture Collection (ATCC, # 14948).

**Surface Functionalization of Substrates with Pyridinium Groups.** The process of functionalizing the substrates with pyridinium groups is indicated in Scheme 1. These steps are described in detail below.

(a) *Argon Plasma Pretreatment.* The PET film or filter paper was cut into strips of 2.5 cm  $\times$  5 cm in size. The PET film was cleaned with absolute ethanol for 5 min in an ultrasonic water bath. The substrates were then subjected to argon plasma pretreatment in an Anatech SP100 plasma system, equipped with a cylindrical quartz reactor chamber. The glow discharge was produced at a plasma power of 35 W, an applied oscillator frequency of 40 kHz and an argon pressure of approximately 0.6 Torr. The substrate was placed between the two electrodes and each surface was subjected to glow discharge for 30 s, which was earlier found to be an optimal condition for the grafting procedure.<sup>17</sup> After plasma pretreatment of both surfaces, the substrate was exposed to air for 5–10 min to facilitate the formation of surface oxide and peroxide groups before graft copolymerization was carried out.<sup>18</sup>

(b) *Surface Graft Copolymerization with 4VP.* The plasma-pretreated substrates were immersed in 2-propanol solutions of 4VP of a predetermined concentration between 1 and 20 vol % in a Pyrex glass tube. Degassing of the solutions was achieved by bubbling nitrogen vigorously into the solution for 30 min before stoppering and sealing the tubes with silicon rubber stoppers. The substrates in the 4VP solution at 25  $^{\circ}\text{C}$  were then exposed

to UV irradiation in a Riko rotary photochemical reactor (RH400-10W) for 60 min on each surface. The graft-copolymerized substrates were finally subjected to washing with copious amounts of ethanol to remove the residual monomer and physically adsorbed homopolymer.<sup>19</sup>

(c) *Quaternization of the Graft-Copolymerized 4VP.* The substrates with graft-copolymerized 4VP were then placed in 30 mL solutions of nitromethane containing 20 vol % hexyl bromide and the reaction mixture was stirred for 48 h at 70  $^{\circ}\text{C}$ .<sup>10,20</sup> At the end of the reaction period, the substrates were thoroughly rinsed with nitromethane to remove the unreacted substances and then dried under reduced pressure.

**Surface Analysis.** (a) *XPS Characterization.* XPS analysis of the substrate was made on an AXIS HSi spectrometer (Kratos Analytical Ltd.) using the monochromatized Al K $\alpha$  X-ray source (1486.6 eV photons) at a constant dwell time of 100 ms and a pass energy of 40 eV. The anode voltage was 15 kV, and the anode current was 10 mA. The pressure in the analysis chamber was maintained at  $5.0 \times 10^{-8}$  Torr or lower during each measurement. The substrates were mounted on standard sample studs by means of double-sided adhesive tape. The core-level signals were obtained at a photoelectron takeoff angle of 90 $^{\circ}$  (with respect to the sample surface). To compensate for surface charging effect, all core-level spectra were referenced to the C 1s hydrocarbon peak at 284.6 eV. In spectral deconvolution, the line width (full width at half-maximum) of the Gaussian peaks was maintained constant for all components in a particular spectrum. The peak area ratios for the various elements were corrected using experimentally determined instrumental sensitivity factors.

(b) *Titration of Pyridinium Groups on PET Film Surfaces.* The PET films after surface functionalization were immersed in a 1% fluorescein (Na salt) solution in distilled water for 5 min with constant shaking, followed by thoroughly rinsing with doubly distilled water. The stained film was then placed in an aqueous solution of 0.25 wt % cetyltrimethylammonium chloride and the mixture was shaken for 10 min to desorb the dye. A 0.1 M aqueous phosphate buffer, pH 8.0, was then added in a ratio of 1 part buffer to 9 parts of cetyltrimethylammonium chloride solution and the absorbance of the resultant solution was measured at 501 nm. The amount of dye bound to pyridinium groups on the film surface was calculated on the basis of a standard calibration. The corresponding pyridinium concentration was then calculated based on the assumption of one dye molecule per seven hexyl-PVP monomeric units.<sup>10</sup>

**Determination of Antibacterial Characteristics.** *E. coli* was cultivated in 50 mL of a 3.1% yeast–dextrose broth (containing 10 g/L peptone, 8 g/L beef extract, 5 g/L sodium

(17) Ying, L.; Yin C.; Zhuo, R. X.; Leong, K. W.; Mao, H. Q.; Kang, E. T.; Neoh, K. G. *Biomacromolecules* **2003**, *4*, 157.

(18) Suzuki, M.; Kashida, A.; Iwata, H.; Ikada, Y. *Macromolecules* **1986**, *19*, 1804.

(19) Yang, G. H.; Kang, E. T.; Neoh, K. G. *Langmuir* **2001**, *17*, 211.

(20) Biesalski, M.; R  he, J. *Macromolecules* **1999**, *32*, 2309.

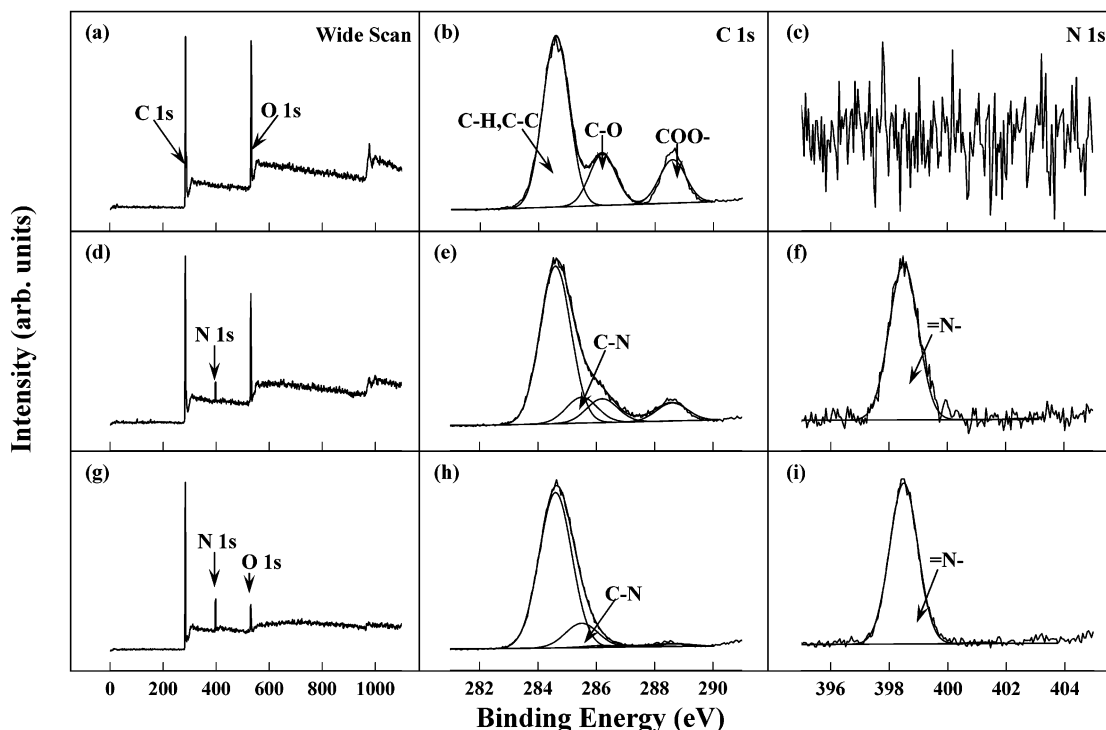


**Figure 1.** XPS wide scan, C 1s and N 1s core-level spectra of (a–c) pristine PET film, (d–f) PET film after UV-induced graft copolymerization with 4VP using 5 vol % monomer in 2-propanol, and (g–i) PET film after UV-induced graft copolymerization with 4VP using 20 vol % monomer in 2-propanol.

chloride, 5 g/L glucose, and 3 g/L yeast extract at a pH of 6.8)<sup>21</sup> at 37 °C. The bacterial cell concentration was measured by the optical density at 540 nm and the cell number was calculated based on the standard calibration with the assumption that the optical density of 1.0 at 540 nm is equivalent to approximately  $10^9$  cells/mL.<sup>22</sup>

For the airborne antibacterial assay, the *E. coli*-containing broth was centrifuged at 2700 rpm for 10 min, and after the removal of the supernatant, the cells were washed with doubly distilled water and resuspended in doubly distilled water at a concentration of  $10^7$  cells/mL. The substrates (PET film or filter paper) were then sprayed with the bacterial suspension using a commercial chromatography sprayer. After several minutes of drying in air, the substrates were placed in Petri dishes. The Petri dishes were then sealed with growth agar (0.7% agar in yeast–dextrose broth, autoclaved, and cooled to 37 °C) and incubated at 37 °C for 24 h.<sup>11</sup>

For the waterborne antibacterial assay, the *E. coli*-containing broth was centrifuged at 2700 rpm for 10 min, and after the removal of the supernatant, the cells were washed twice with PBS (pH 7.0) and resuspended in PBS at a concentration of  $10^7$  cells/mL. The substrates were immersed in this suspension in a sterile Erlenmeyer flask. The flask was then shaken at 200 rpm at 37 °C for 2 h. The substrates were then removed from the above flask and washed three times with sterile PBS and placed in Petri dishes. This was followed by the immediate addition of solid growth agar (1.5% agar in yeast–dextrose broth, autoclaved, poured into a Petri dish, and dried under reduced pressure at room-temperature overnight). The Petri dishes were then sealed and incubated at 37 °C for 24 h.<sup>11</sup>

The substrates after the airborne or waterborne antibacterial assays were characterized by either optical microscopy (using an Olympus BX60) or scanning electron microscopy (SEM). The sample fixation and preparation for SEM were as follows: the substrates were first washed with PBS immediately after the incubation period and 3 vol % glutaraldehyde in PBS was added for 5 h and stored at 4 °C. The glutaraldehyde solution was then

removed and the substrates were washed with PBS, followed by step dehydration with 25%, 50%, 70%, 95%, and 100% ethanol for 10 min each. The substrates were then dried and sputter-coated with a thin film of platinum for imaging purposes. The SEM characterization was carried out on a JEOL JSM 5600LV scanning electron microscope.

**Adhesion and Viability Assay of Bacteria on PET Substrates.** The PET substrates were immersed in a PBS (pH 7.0) suspension of  $10^7$  cells/mL in a sterile Erlenmeyer flask. The flask was then shaken at 200 rpm at 37 °C for either 5 min or 2 h. After that, the substrates were taken out and washed extensively with sterile PBS. Sterilized filter paper was used to suck up the moisture on the substrate surface, after which the substrates were immersed into a yeast–dextrose broth.<sup>23</sup> After being cultured at 37 °C for 24 h, the substrates were removed and the optical density at 540 nm of the broth was then observed. Control experiments were made with the pristine PET substrate and the optical densities were compared. The substrates before and after culturing in the yeast–dextrose broth were also examined under SEM to assess how the adhesion and viability of the bacteria were affected by the presence of the pyridinium groups.

## Results and Discussion

**1. Surface Graft Copolymerization of PET Films with 4VP.** The success of the UV-induced surface graft copolymerization of 4VP on the PET film can be ascertained by comparing the XPS spectra of the films before and after the grafting process (Figure 1). The XPS C 1s core-level spectrum of the pristine PET film (Figure 1b) shows a predominant peak component at the binding energy (BE) of 284.6 eV due to the aromatic carbon, and two peak components at BEs of 286.2 and 288.6 eV due to singly bonded CO and carboxyl carbon (COO<sup>−</sup>), respectively. The areas of the three peak components are approximately in a ratio of 3:1:1 which is in good agreement with the chemical structure of PET.<sup>24</sup> Since there is no nitrogen in the PET structure, no nitrogen component

(21) Cunliffe, D.; Smart, C. A.; Alexander, S.; Vulfson, E. N. *Appl. Environ. Microbiol.* **1999**, *65*, 4995.

(22) Hogt, A. H.; Dankert, J.; Feijen, J. J. *Biomed. Mater. Res.* **1986**, *20*, 533.

(23) Li, G.; Shen, J. J. *J. Appl. Polym. Sci.* **2000**, *78*, 676.



**Table 1. Surface Composition of PET after 4VP Functionalization and Hexyl Bromide Derivatization**

substrate	4VP monomer concentration (vol %) used for surface graft copolymerization	surface [N]/[C] ratio <sup>a</sup> after 4VP graft copolymerization	surface [N <sup>+</sup> ]/[C] ratio <sup>a</sup> after hexyl bromide derivatization	pyridinium concentration ([N <sup>+</sup> ]) on modified film surfaces (nmol/cm <sup>2</sup> ) <sup>b</sup>
PET	0	0	0	0
P-1	1	0.010	0.0049	0.11
P-2.5	2.5	0.031	0.0098	0.79
P-5	5	0.053	0.014	2.41
P-10	10	0.079	0.027	15.0
P-20	20	0.11	0.032	19.8

<sup>a</sup> As determined by XPS. <sup>b</sup> As determined by fluorescein staining.

can be detected as shown in Figure 1c. The presence of the surface grafted 4VP polymer after the UV-induced graft copolymerization step can be deduced from the wide scan (Figure 1d), which shows the presence of the N 1s peak at around 400 eV. The corresponding N 1s spectrum (Figure 1f) shows an intense peak at the BE of 398.5 eV attributable to the imine moiety ( $\text{--N=}$ ) of the pyridine rings.<sup>19</sup> The C 1s core-level spectrum after 4VP grafting (Figure 1e) shows an additional peak at 285.5 eV attributable to the C–N species and a decrease in the intensity of the CO and COO<sup>–</sup> peak components as compared with Figure 1b. As the surface coverage of the 4VP copolymer increases with increasing 4VP monomer concentration used in the grafting process, the intensity of the peaks assigned to CO and COO<sup>–</sup> species became increasingly weaker until the peaks are no longer discernible (Figure 1h). Similarly, as the 4VP surface graft concentration increases, the intensity of the N 1s signal increases relative to the O 1s signal (Figure 1g).

The concentration of quaternary ammonium groups which have effective antibacterial properties depends on the concentration of the pyridine groups from 4VP graft copolymerized on the surface. The extent of surface grafting of 4VP can be estimated from the sensitivity factor corrected ratio of the total N 1s peak over the total C 1s peak, and expressed as [N]/[C]. The change in the surface graft concentration of the 4VP polymer with the monomer concentration used for graft copolymerization is shown in Table 1. It can be seen that the surface [N]/[C] ratio increases with 4VP monomer concentration. At a monomer concentration of 20 vol %, the ratio of 0.11 is close to the value of 0.14, expected for the 4VP monomeric unit ( $\text{C}_7\text{H}_7\text{N}_1$ ). This indicates that the surface is almost completely covered by 4VP copolymers to a depth of  $\sim 8$  nm which is the probing depth of the XPS technique for an organic matrix.<sup>25</sup>

## 2. Quaternization of Graft-Copolymerized 4VP.

The conversion of the N-pyridine rings to pyridinium groups after reaction with hexyl bromide were investigated using XPS and fluorescein titration. Figure 2 shows the XPS spectra of the surface derivatized PET film which was first grafted with 20 vol % 4VP and subsequently N-alkylated with hexyl bromide. No significant difference can be observed in C 1s core-level spectrum before (Figure 1h) and after (Figure 2a) the alkylation process except for the appearance of a small peak component at the BE of 286.2 eV, attributable to the CO species. It is unlikely that this peak is due to the loss of the 4VP graft copolymers from the surface which would result in the exposure of the underlying PET film surface, since PET has equal amounts of CO and COO<sup>–</sup> species, and there was no

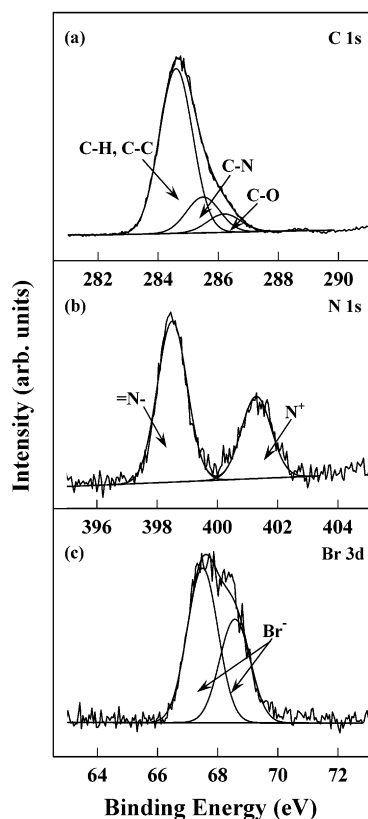


**Figure 2.** XPS (a) C 1s, (b) N 1s, and (c) Br 3d core-level spectra of PET film after UV-induced graft copolymerization with 4VP in 20 vol % monomer in 2-propanol and subsequently derivatized with 20 vol % hexyl bromide in nitromethane.

evidence of COO<sup>–</sup> species in Figure 2a. Hence the CO species may be due to oxidation of a trace amount of the carbon species on the surface during the alkylation reaction.

The corresponding N 1s core-level spectrum in Figure 2b shows an additional peak at a binding energy above 400 eV, attributable to the N<sup>+</sup> groups of the pyridinium ions.<sup>26</sup> This confirms the derivatization of the  $\text{--N=}$  groups by hexyl bromide. On the basis of the [N<sup>+</sup>]/[N] ratio, the degree of alkylation of the pyridine rings is around 30–40%. In the Br 3d core-level spectrum (Figure 2c) the presence of a doublet (Br 3d<sub>5/2</sub> and Br 3d<sub>3/2</sub>) at 67.5 and 68.6 eV attributable to Br<sup>–</sup> species<sup>27</sup> further confirms the reaction between the 4VP graft copolymer on the PET film surface and hexyl bromide. The [N<sup>+</sup>]/[C] ratio of the PET substrate with different extents of 4VP graft copolymer after hexyl bromide derivatization is shown in Table 1. As expected, with a higher amount of 4VP

(24) Loh, F. C.; Tan, K. L.; Kang, E. T.; Uyama, Y.; Ikada, Y. *Polymer* **1995**, *36*, 21.

(25) Briggs, D. *Surface Analysis of Polymers by XPS and Static SIMS*; Cambridge University Press: New York, 1998; p 39.

(26) Tan, K. L.; Tan, B. T. G.; Kang, E. T.; Neoh, K. G. *J. Mol. Electron.* **1990**, *6*, 5.

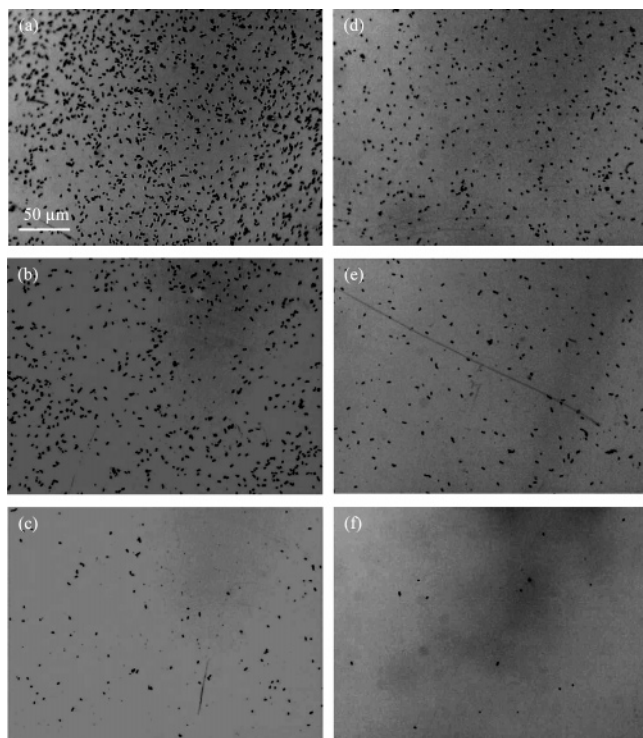


**Figure 3.** Optical micrographs of (a and d) pristine PET, (b and e) P-1, and (c and f) P-10 surfaces after exposure to airborne and waterborne *E. coli*, respectively, and subsequent incubation in solid growth agar for 24 h.

copolymers present on film surface, the concentration of pyridinium groups is higher. The quantitative amount of  $[N^+]$  present on the corresponding film surfaces as obtained from the titration method using fluorescein (Na salt) is also shown in Table 1. Previous work has shown that this dye only binds to quaternary amino groups but not tertiary or primary ones.<sup>28</sup> Our control experiments with pristine PET film and PET films with various amounts of 4VP grafted but not derivatized also confirmed that fluorescein (Na salt) only binds to quaternary amino groups. The results in Table 1 show that the amount of surface  $[N^+]$  increases by over 2 orders of magnitude as the amount of 4VP monomer concentration used in the grafting process increases from 1 to 10 vol %. Further increase in monomer concentration beyond this value results in only an incremental increase in  $[N^+]$ . This effect may be due to steric hindrance which limits the approach of the hexyl bromide molecules to the pyridine groups. As will be illustrated below, the antibacterial efficiency of the film is highly dependent on the amount of quaternary ammonium groups on the surface.

**3. Antibacterial Characteristics of Functionalized PET.** Both airborne and waterborne tests were performed to simulate the natural deposition of *E. coli* on substrates. Three substrates were chosen for these tests: pristine PET film; PET film which was graft copolymerized with 1 vol % 4VP monomer concentration and subsequently quaternized with hexyl bromide (P-1 in Table 1); PET film obtained under the same conditions except the monomer concentration used was 10 vol % (P-10 in Table 1). Figure 3 shows the optical microscopy results of the PET films after airborne and waterborne antibacterial tests. In Figure 3a, numerous distinguishable bacteria colonies can be observed on the pristine PET surface. The

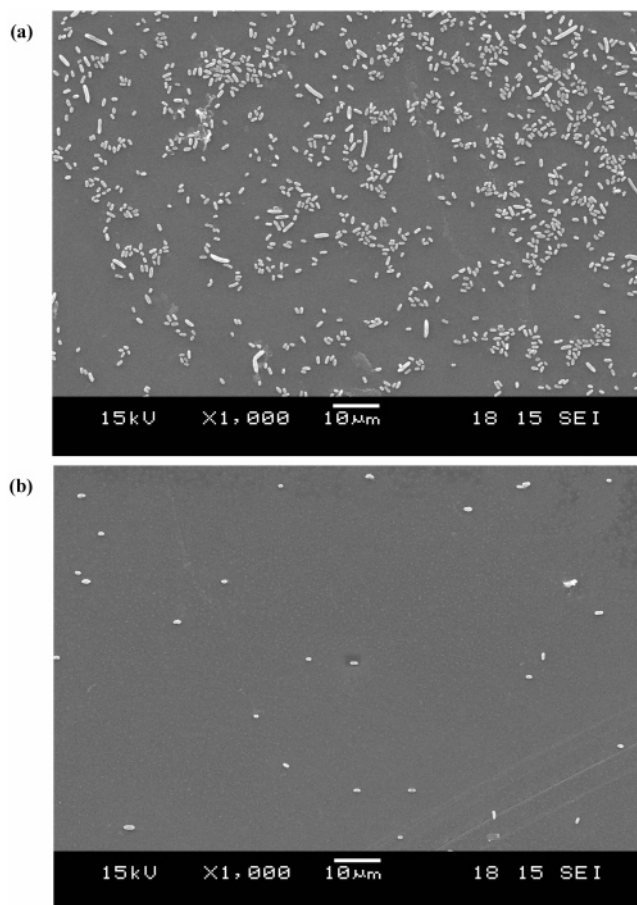


**Figure 4.** Scanning electron micrographs of (a) PET and (b) P-10 films after exposure to airborne *E. coli* and subsequent incubation with solid growth agar for 24 h.

number of colonies on the P-1 surface as shown in Figure 3b is significantly less, and this decrease was even more substantial for the P-10 surface (Figure 3c). Control experiments conducted with PET films grafted with 1 and 10 vol % 4VP but without subsequent derivatization gave results similar to that obtained with the pristine PET film. A similar trend showing the effectiveness of the functionalized surfaces in preventing *E. coli* growth can be observed in the waterborne tests (Figure 3d–f). The importance of having a high concentration of  $[N^+]$  to achieve effective antibacterial activities is thus clearly demonstrated in both the airborne and waterborne tests.

A difference observed between the airborne and waterborne tests is the higher concentration of colonies on the corresponding substrates in the former. This may be due to the fact that in the airborne tests the bacteria were sprayed directly on the different substrates whereas for the waterborne tests, only the bacteria which adhered to the substrates after their removal from the suspension were considered. The issue of whether the surface groups affect the adhesion of the bacteria in the waterborne test would be addressed in greater detail in a later section.

The SEM micrographs of the pristine PET and P-10 substrates after the above-mentioned airborne test are shown in Figure 4. These micrographs show a clear difference between the *E. coli* on the PET and P-10 substrates. In addition to the substantially higher concentration of bacteria on the pristine PET, the bacteria on this surface also show active cell growth and division. A number of the bacteria cells are between 2 and 6  $\mu\text{m}$  in length. In contrast, the *E. coli* on the P-10 substrate (Figure 4b) is sparsely distributed as single cells of the order of

(27) Zhao, B.; Neoh, K. G.; Kang, E. T. *Chem. Mater.* **2000**, *12*, 1800.

(28) Ledbetter, J. W., Jr., & Bowen, J. R. *Anal. Chem.* **1969**, *41*, 1345.



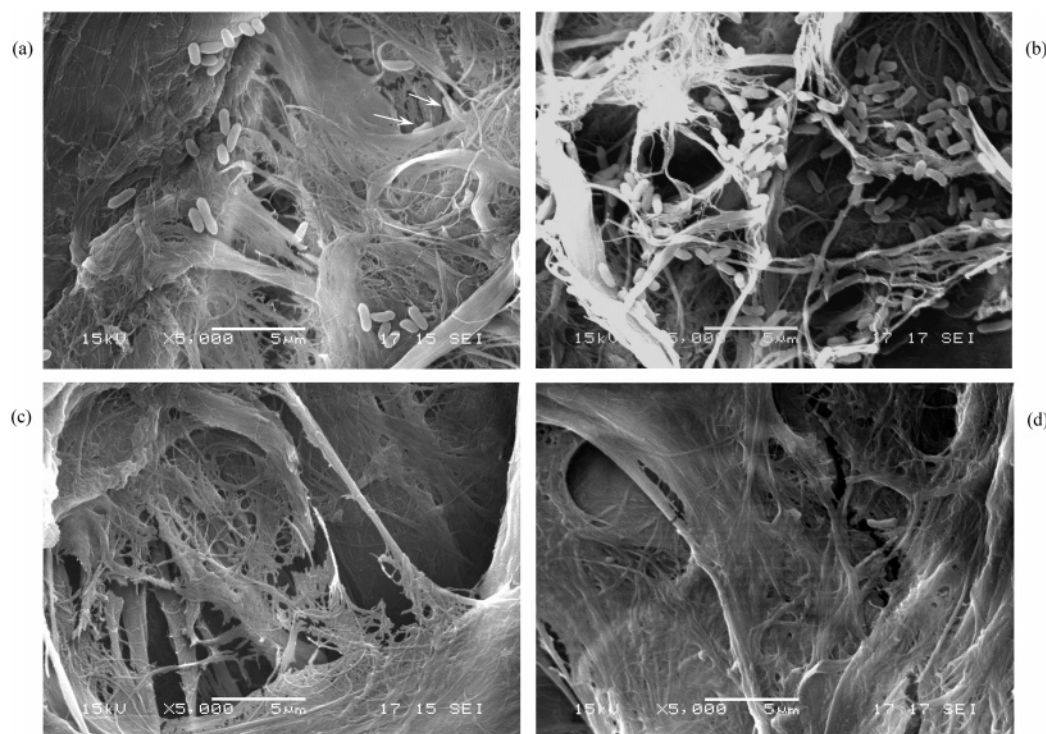


**Figure 5.** Scanning electron micrographs of FP after exposure to airborne (a) and waterborne (b) *E. coli*, respectively, and subsequent incubation with solid growth agar for 24 h and FP-10 after exposure to airborne (c) and waterborne (d) *E. coli*, respectively, and subsequent incubation with solid growth agar for 24 h.

1  $\mu\text{m}$  in length. There is no evidence of growth or reproduction. The results confirm that normal polymer slides are good templates for the proliferation of microorganisms and biofilm formation occurs readily on such polymeric surfaces in contact with bacteria.<sup>29,30</sup> The presence of quaternary ammonium groups attached to a hexyl group at a surface concentration of 15 nmol/cm<sup>2</sup> is thus demonstrated to be very effective in preventing such a biofilm formation.

**4. Cellulosic Surface Functionalization and Antibacterial Assay.** The functionalization technique developed for the PET substrate was applied to commercial filter paper (Whatman Grade 1 filter paper was chosen as it is the most widely used filter paper in the Whatman range). XPS studies (results not shown) also confirm the success of the surface functionalization procedures for this substrate. From SEM micrographs of the filter paper before and after surface functionalization, it can be concluded that the filter paper did not show significant changes in its morphology and structure during the course of the surface functionalization.

The pristine filter paper, denoted as FP, and the 4VP grafted (using 10 vol % 4VP monomer) and hexyl bromide derivatized filter paper, denoted as FP-10, were assayed with airborne and waterborne antibacterial tests as described in the Experimental Section. The SEM micrographs of the substrates after the airborne and waterborne tests are shown in Figure 5. Figure 5a shows the FP after the airborne tests. The *E. coli* was distributed not only on the FP upper surface but also entrapped in the space among the fibers as indicated by the arrows in Figure 5a. After the waterborne tests, numerous bacteria could be seen to grow in the interstitial spaces and along the thin fibers of FP (Figure 5b). More bacteria could be seen to grow on FP after the waterborne test (Figure 5b) compared

with those on FP after the airborne test (Figure 5a). This phenomenon is in contrast to the results obtained for the pristine PET substrate after the airborne and waterborne tests (Figure 3, parts a and d). The reason lies in the difference between porous and nonporous substrates. Since the interstitial spaces of the filter paper are large enough for bacteria to penetrate into, it can be expected that some bacteria would have penetrated deep into the filter paper during the immobilization procedure of the waterborne test which lasts for 2 h. Therefore, the larger concentration of bacteria entrapped in the porous matrix during the waterborne test before the subsequent incubation with growth agar results in a denser population of bacteria growing on FP as shown in Figure 5b.

In the case of the FP-10 after the airborne test, very few sparsely distributed bacteria cells can be spotted over the entire surface (Figure 5c). A similar observation was obtained for the FP-10 substrate after the waterborne test (Figure 5d). In contrast to the clumps of bacteria seen in Figure 5b, only few single cells can be spotted among the fibers in Figure 5d. Hence, the results obtained using the functionalized filter paper confirm the applicability of the technique to high surface area porous materials and similar high efficiency of antibacterial action is obtained upon contact for both the porous and nonporous materials.

**5. Adhesion and Viability Assay of Cells Adhered on Polymeric Film Surfaces.** This assay was intended to address the issue of whether the surface groups on the modified PET affected the initial adhesion of the bacteria during the waterborne tests. In addition, it would be of interest to elucidate whether cells adhered to the functionalized substrate for a short period of time remained viable when released into a fresh culture medium. In these adhesion and viability tests, the procedures were similar to the procedures for the waterborne test as described earlier except that solid growth agar was not applied on the substrates. Instead, the substrates with adhered bacteria were either immediately sent for SEM charac-

(29) Costerton, J. W.; Stewart, P. S.; Greenberg, E. P. *Science* **1999**, *284*, 1318.

(30) Lewis, K. *Antimicrob. Agents Chemother.* **2001**, *45*, 999.

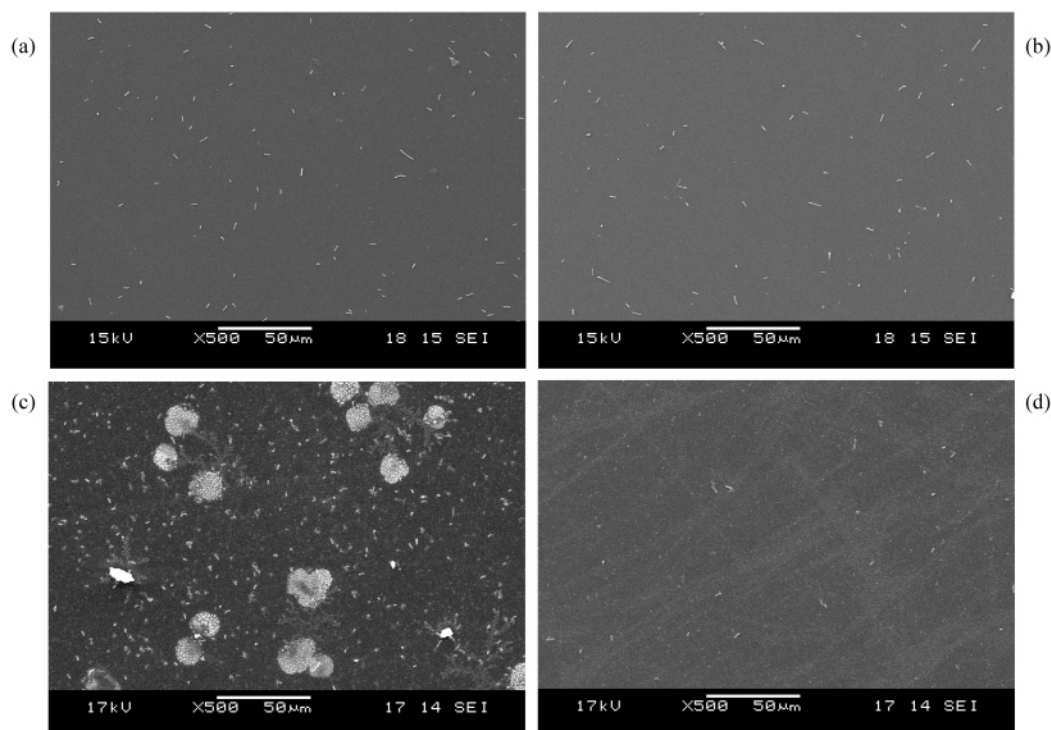


**Figure 6.** Scanning electron micrographs of (a) pristine PET and (b) P-10 surfaces after exposure to a PBS suspension of  $10^7$  cells/mL *E. coli* for 2 h and (c) pristine PET and (d) P-10 film surfaces after exposure to a PBS suspension of  $10^7$  cells/mL *E. coli* for 2 h and subsequent reculturing in yeast–dextrose broth for 24 h.

terization or recultured in 45 mL of yeast–dextrose broth in a sterile Erlenmeyer flask at 37 °C for 24 h with constant shaking. The SEM micrographs of the PET and P-10 substrates after the initial immersion in the cell suspension (of  $10^7$  cells/mL) for 2 h are shown in Figure 6, parts a and b, respectively. The immersion time of 2 h was chosen to facilitate the metabolic recovery of bacteria from a suspension to a substrate.<sup>31</sup> No significant difference in the quantity and distribution of the attached bacteria on the two surfaces can be observed from the SEM micrographs. The microbial adhesion to different substratum surfaces is known to be affected by the various chemical and physicochemical factors of the substrate under the same environmental conditions, such as hydrophobicity or hydrophilicity,<sup>32</sup> steric hindrance,<sup>33</sup> roughness,<sup>34</sup> and the existence of a “conditioning layer”<sup>35</sup> at the substrate surface. It is often the collaboration of those factors that contributes to the initial cell attachment process. In the present work, both the PET and P-10 surfaces are quite hydrophobic as the water contact angle of pristine PET is more than 70° and that of P-10 is around 70°, as measured by a telescopic goniometer (Rame-Hart, model 100-0-230). Furthermore, the root-mean-square surface roughness of the pristine PET and P-10 surfaces as measured by atomic force microscopy (measurement area of 10  $\mu\text{m}$ ) is about 1.67 and 3.57 nm respectively. Although it has been reported that the surface hydrophobicity and roughness enhances bacteria attachment,<sup>32</sup> the differences in hydrophobicity and roughness between the PET and P-10 surfaces are not expected to contribute

to a significant difference in bacteria adhesion, and this is confirmed by the SEM micrographs in Figure 6, parts a and b.

Another factor to consider is the negatively charged nature of the bacteria surface. It may be expected that the interaction between the bacteria and the positively charged pyridinium groups on the P-10 surface is stronger than with PET which is an inert substratum. However, it has also been reported that interaction forces include the ever present Lifshitz–van der Waals forces, electrostatic forces, and acid–base interactions,<sup>36</sup> and all these nonspecific forces act together in cell adhesion or repulsion. Moreover, each interaction force might be constrained by its specific operative distance.<sup>37</sup> As this assay was carried out in an aqueous suspension with shaking at a high speed (200 rpm), the hydrodynamic forces are also believed to be important. Hence, the association between a microorganism and a substratum surface that contributes most to the microbial adhesive interactions is believed to be a dynamic process which takes some time to achieve equilibrium. In the present work, adhesion assays using the substrates in suspensions of different bacteria concentrations were compared. With a bacteria concentration of  $10^9$  cells/mL in the suspension, substantially more bacteria was observed to adhere on the PET and P-10 substrates compared to the results shown in Figure 6, parts a and b, which were obtained with a suspension of  $10^7$  cells/mL. However, there is still no significant difference between the amounts of adhered bacteria on the two different substrates. Therefore, the concentration of the bacteria adhered on the different substrates is affected more by the concentration in the suspension than the presence of the positively charged pyridinium groups of the concentration used in our experiments.

(31) Arnold, J. W.; Silvers, S. *Poultry Sci.* **2000**, *79*, 1215.

(32) Reid, G.; Lam, D.; Policova, Z.; Neumann, A. W. *J. Mater. Sci.—Mater. Med.* **1993**, *4*, 17.

(33) Kuhl, T. L.; Leckband, D. E.; Lasic, D. D.; Israelachvili, J. N. *Biophys. J.* **1994**, *66*, 1479.

(34) Arnold, J. W.; Bailey, G. W. *Poultry Sci.* **2000**, *79*, 1839.

(35) Abarzua, S.; Jakubowski, S. *Mar. Ecol.: Prog. Ser.* **1995**, *123*, 301.

(36) Van Oss, C. J. *Mol. Immunol.* **1995**, *32*, 199.

(37) Bos, R.; van der Meu, H. C.; Busscher, H. J. *FEMS Microbiol. Rev.* **1999**, *23*, 179.



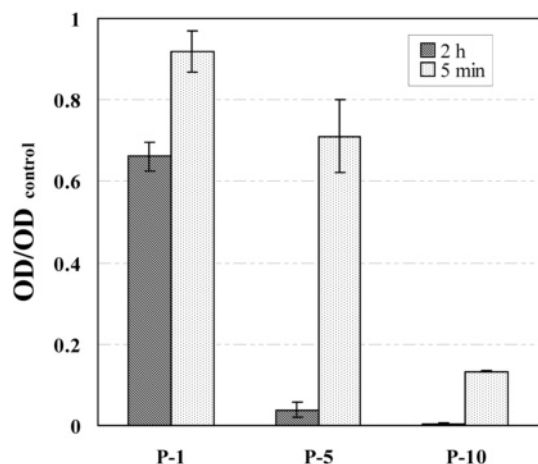


**Figure 7.** Normalized optical densities at 540 nm of nutrient broth after 24 h in contact with P-1, P-5, and P-10 surfaces with adhered *E. coli*. The substrates were initially immersed in an *E. coli* suspension of  $10^7$  cells/mL for either 2 h or 5 min before transferring to the nutrient broth. OD<sub>control</sub> is the optical density obtained using pristine PET as the substrate in the experiment.

The SEM micrographs of the pristine PET and P-10 substrates with adhered bacteria after reculturing for 24 h are shown in Figure 6, parts c and d. As can be seen from Figure 6c, the surface of the pristine PET substrate was bestrewn with bacteria in the form of big colonies, which may lead to the formation of a biofilm. On the other hand, the bacteria present on the P-10 surface after reculturing (Figure 6d) remained as single cells in a very sparse distribution, similar to that observed before reculturing (Figure 6b). The SEM micrographs of both the PET and P-10 surfaces after reculturing (Figure 6, parts c and d) show the presence of a thin film. This film is the result of adsorption of organic matters present in the yeast–dextrose broth and is generally referred to as “conditioning film”.<sup>38</sup>

After the substrates were removed from the nutrient broth, the optical density of the broth was measured at 540 nm to obtain an indication of the bacteria concentration. The results from the experiments using four different substrates, pristine PET, P-1, P-5, and P-10, are compared in Figure 7. In this figure, the optical density obtained from the nutrient broth with the three functionalized PET substrates was normalized to that obtained with the pristine PET film. For the series of experiments carried out with the substrates initially immersed for 2 h in the *E. coli* suspension, the optical densities of the medium with the P-1, P-5, and P-10 substrates are about 70%, 5%, and <1% of that obtained with the pristine PET control, respectively. Therefore, it can be concluded that the adhered bacteria on the pristine PET substrate not only grows well on the substrate surface, but upon release from the substrate into an aqueous medium, it remains viable and reproduces in the medium. However, the P-10 surface is highly detrimental to the bacteria upon contact and the bacteria cells released into growth medium are no longer viable. The importance of having a sufficiently high concentration of pyridinium groups ( $\sim 15$  nmol/cm<sup>2</sup>) is also illustrated since the same bacteria released from the P-1 and P-5 substrates continued to multiply in the growth medium.

To further investigate the effect of time on bacteria adhesion and destruction, the experiments were also carried out for substrates immersed in the same bacteria

suspensions for 5 min instead of 2 h. The optical density of the nutrient broth cultured with the pristine PET which was immersed for 5 min in the bacterial suspension was about 30% of the value obtained with a 2 h immersion period (not shown). As a low optical density is equivalent to a low bacteria concentration in the medium, it is clear a short contact time of 5 min results in less bacteria adhering to the substrate and subsequently transferring to the culture broth. The higher concentration of bacteria adhered on the pristine PET and P-10 substrates after 2 h as compared to 5 min immersion in the bacteria suspension is confirmed by SEM investigation of the substrates after removal from the suspension. The resultant optical densities of the nutrient broth for the series of experiments carried out with the 5 min immersion time are also shown in Figure 7. The optical densities in this series are normalized with respect to the corresponding value obtained with the pristine PET as the control. In this case, the optical densities of the medium with the P-1, P-5, and P-10 substrates are about 90%, 70%, and 15% respectively of that obtained with the corresponding pristine PET control. From Figure 7, it can be seen that for any substrate the normalized optical density obtained from the 5 min immersion experiments is higher than the corresponding value from the 2 h immersion experiments. This observation indicates that not only is the adhesion of bacteria to the substrates time-dependent, but it may also take time for the *N*-hexylpyridinium groups to be effective in killing the *E. coli*. Nevertheless, as shown in Figure 7, the P-10 substrate is still very effective in killing *E. coli* on contact even for a period of time as short as 5 min.

The bactericidal ability of the surface-attached polycationic chains have been attributed to the penetration of those polycationic chains into the bacterial membrane resulting in the cell damage and death.<sup>10–12</sup> The following sequential steps have been proposed for this mechanism: (1) adsorption of positively charged polycations onto the negatively charged cell surfaces, (2) penetration into the cell wall, (3) binding to the cytoplasmic membrane, (4) disruption of the cytoplasmic membrane, (5) release of K<sup>+</sup> ions and constituents of the cytoplasmic membrane, and (6) death of the cell.<sup>39</sup> The present work further confirms the antibacterial activity of surface-attached polycationic *N*-hexyl chains, but in order to achieve high killing efficiency, sufficiently high concentration of the polycationic groups is needed. The present technique allows for good control of the concentration of the functional groups and is applicable to both polymeric and cellulosic materials.

## Conclusion

Commercial PET films and filter paper can readily undergo UV-induced surface graft copolymerization with 4VP, and the subsequent alkylation of the grafted 4VP groups to yield the pyridinium groups. The 4VP graft concentration can be controlled by varying the monomer concentration used in the grafting process and is a key factor in determining the amount of surface functional groups available for quaternization. Both airborne and waterborne assays with *E. coli* show that the polycationic chains introduced on the substrate surface via derivatization of the pyridine groups by hexyl bromide possess the desired antibacterial activity. The bacteria killing efficiency is dependent on the surface pyridinium concentration and a surface concentration of 15 nmol/cm<sup>2</sup> on

(38) Gristina, A. G. *Science* **1987**, 237, 1588.

(39) Tashiro, T. *Macromol. Mater. Eng.* **2001**, 286, 63.



PET has been shown to be highly effective. At this concentration, the *E. coli* bacteria is rapidly killed on contact, and very few cells remain viable even after release into growth medium. The functionalization technique developed in this work has the advantage of ease of application to different types of substrates and offers the

flexibility in altering the type and concentration of the surface functional groups. Further work in progress involves the investigation of the effects of different functional groups and microorganisms.

LA035104C